Combined experimental and theoretical study on the effect of Nb content on martensitic transformation of NbRu shape memory alloys*

Tan Chang-Long(谭昌龙)[a)†], Cai Wei(蔡 伟)[b)], and Tian Xiao-Hua(田晓华)[a)]

[a)] College of Applied Science, Harbin University of Science and Technology, Harbin 150080, China
[b)] School of Materials Science and Engineering, Harbin Institute of Technology, Harbin 150001, China

(Received 22 April 2009; revised manuscript received 15 September 2009)

The effect of Nb content on the martensitic transformation of NbRu high-temperature shape memory alloys is investigated by experiments and first-principles calculations. We calculate the lattice parameters, density of states, charge density, and heats of formation of $Nb_{50+x}Ru_{50-x}$ β phase. The results show that an increase in Nb content increases the stability of $Nb_{50+x}Ru_{50-x}$ β phase, leading to a significant decrease of the β to β' martensitic transformation temperature. In addition, the mechanism of the effects of Nb content on phase stability and martensitic transformation temperature is studied on the basis of electronic structure.

Keywords: high-temperature shape memory alloy, NbRu, electronic structure, martensitic transformation

PACC: 7115A, 7115M, 8130K

1. Introduction

Shape memory alloys (SMAs) have attracted increasing attention due to their shape memory effect (SME) and superelasticity, which are displayed during martensitic transformations.[1] In recent years, SMAs have been widely used as actuators, sensors and medical devices.[2−4] Although many kinds of alloys exhibit the shape memory effect, only TiNi and Cu-base SMAs have been used for commercial purposes. The operating temperatures of SMAs depend on their martensitic transformation temperatures. However, the martensitic transformation temperatures of TiNi and Cu-base alloys are below 150°.[5−7] So they are not able to satisfy the requirements for high-temperature SMAs applications, such as automotive engine, gas turbine and nuclear reactor environments, which require higher martensitic transformation temperatures.[6] Therefore, it is necessary to develop high-temperature SMAs. Nowadays, NbRu alloys demonstrate both martensitic transformation temperature above 900° and the shape memory effect, which makes them attractive candidates for SMAs used at high temperatures.[8−10] The phase transformations in this compound have been studied for over 35 years.[11−15] It is observed that these alloys undergo two displacive transformations both leading to equilibrium phases. Above 900°, the crystal structure is the ordered cubic CsCl-type ($Pm\bar{3}m$), called the β phase. Below 900°, the crystal transforms to a tetragonal structure, called the β' phase. This β-to-β' phase transformation is demonstrated to be responsible for the shape memory effects in these alloys.[16] The second transformation gives rise to a monoclinic β'' phase. In addition, their microstructure, shape memory effect and mechanical behaviour have been studied in recent years.[17−21] The shape memory effect in NbRu is demonstrated on sub-sized three point bent test specimens, and 4% recoverable strains is obtained. The study on mechanical behaviour shows that the equiatomic NbRu alloy is brittle at room tenperature. The investigations above were mainly focused on near equiatomic NbRu alloys. On the other hand, the previous studies indicated that the composition of shape memory alloys had significant effects on the martensitic transformation and shape memory effect.[1] However, to our knowledge, there are only a few investigations on the effects of Nb content on martenstic transformation behaviour of NbRu alloys and its mechanism. Therefore, from the application point of view, it is highly desirable to carry out such investigations.

*Project supported by the Youth Top-notch Innovative Talents Program of Harbin University of Science and Technology.
†Corresponding author. E-mail: changlongtan@yahoo.com.cn
© 2010 Chinese Physical Society and IOP Publishing Ltd

In the present paper, we investigate the effect of Nb content on the martenstic transformation of NbRu high-temperature shape memory alloys by experimental and first-principles methods. Furthermore, both the mechanism of the phase stability and the transformation behaviour of $Nb_{50+x}Ru_{50-x}$ alloys are researched on the basis of the electronic structure. In addition, the shape memory effect of $Nb_{50+x}Ru_{50-x}$ alloys is also studied. Experimental and calculational methods are described in Section 2. The martenstic transformation behaviour of $Nb_{50+x}Ru_{50-x}$ alloys and its mechanism are analysed in Section 3. Conclusions are given in the last section.

2. Experimental and calculational methods

Nominal compositions of the experimental material used in this study are $Nb_{50+x}Ru_{50-x}$($x = -3$, 0, 5). Button-shape samples of several grams in weight are prepared with high purity elements melted in an arc-melting furnace in argon atmosphere. All alloys are remelted several times to ensure homogeneity. The martensitic and reverse transformation temperatures M_s, M_f, A_s, A_f are determined by Perkin–Elmer diamond differential scanning calorimetry (DSC). The martensitic transformation temperature is calculated as $(M_s + A_s)/2$. The rate of heating and cooling is 20°/min. X-ray diffraction (XRD) measurements are performed to determine the crystal structure using a Rigaku D/max-rB with Cu Kα radiation.

The shape recovery strain is measured by the thermal expansion method, with Shimizu TAS-100 equipment. A compression test is conducted on a Gleeble 4500 thermal simulation machine, with a compression rate of 1.6×10^{-4} s^{-1}. The heights of the specimens are measured prior to loading, after loading and after heating at above A_f. The pre-strain during compression is defined as $\varepsilon_{pre} = l/l_0$, where Δl is the displacement of the crosshead. The residual strain after unloading (ε_r), permanent strain (ε_p) and strain which recovered due to the shape memory effect (ε_{SME}) are obtained to be $(l_1 - l_0)/l_0 \times 100\%$, $(l_2 - l_0)/l_0 \times 100\%$ and $(l_1 - l_2)/l_1 \times 100\%$, respectively. The recovery ratio (R) is calculated to be $R = \varepsilon_{SME}/(\varepsilon_{SME} + \varepsilon_p) \times 100\%$.

The calculations presented in this study are performed with the CASTEP code,[22] based on the density functional theory, by using Vanderbilt-type ultrasoft pseudopotentials[23]and a plane-wave expansion of the wave functions. We use the generalized gradient approximation (GGA) to describe the exchange and correlation potential. The structure is optimized with the Broyden–Fletcher–Goldfarb–Shanno (BFGS) method, and convergence is assumed to be achieved when the forces on atoms are less than 0.03 eV/Å (1 Å=0.1 nm). A plane-wave cutoff energy of 300 eV is employed. The calculations are conducted by using an (8, 8, 8) Monkhorst–Pack grid. In order to study the phase stability and electronic structure of $Nb_{50+x}Ru_{50-x}$, calculations are performed for $Nb_{50+x}Ru_{50-x}$($x = -6.25$, 0, 6.25) β phases. The crystal structure of the $Nb_{43.75}Ru_{56.25}$ β phase is taken as a $2 \times 2 \times 2$ CsCl-type NbRu supercell, in which body-centred Nb is replaced by Ru. The supercell for the $Nb_{56.25}Ru_{43.75}$ β phase is similar to this, but with body-centred Ru replaced by Nb. The lattice parameters of CsCl-type NbRu are cited from Ref. [24]. In every case, geometrical optimization is always done, based on which the heats of formation, the lattice parameters and the electronic structure are then calculated.

3. Results and discussion

Figure 1 shows the DSC curves of $Nb_{50+x}Ru_{50-x}$ ($x = -3$, 0, 5) alloys. It can be seen that the studied alloys exhibit a two-step martensitic transformation behaviour ($\beta \rightarrow \beta' \rightarrow \beta''$) both in heating and in cooling. The characteristic temperatures of the martensitic transformation of $Nb_{50+x}Ru_{50-x}$ alloys are listed in Table 1. The martensitic and reverse transformation temperatures of β-to-β' are denoted by M_{s1}, M_{f1}, A_{s1}, A_{f1}. The martensitic and reverse transformation temperatures of β'-to-β'' are denoted by M_{s2}, M_{f2}, A_{s2}, A_{f2}.

Figure 2 shows the effect of Nb content on the β-to-β' martensitic transformation temperature (T_m) of $Nb_{50+x}Ru_{50-x}$($x = -3$, 0, 5) alloys. It can be clearly seen that the T_m decreases nearly linearly with increasing Nb content. This indicates that the T_m of NbRu alloys can be adjusted by changing the Nb content, which is considered to be of potential technological interest. Moreover, according to the previous study,[16] the lattices of high-temperature phase, mid-temperature phase and low-temperature phase in NbRu alloys are identified to be of CsCl type, face-centred tetragonal type, monoclinic type (β'' martensite), respectively. For our studied alloys, their T_m is above room temperature, indicating that the crystal structure at room temperature is of β'' martensite.

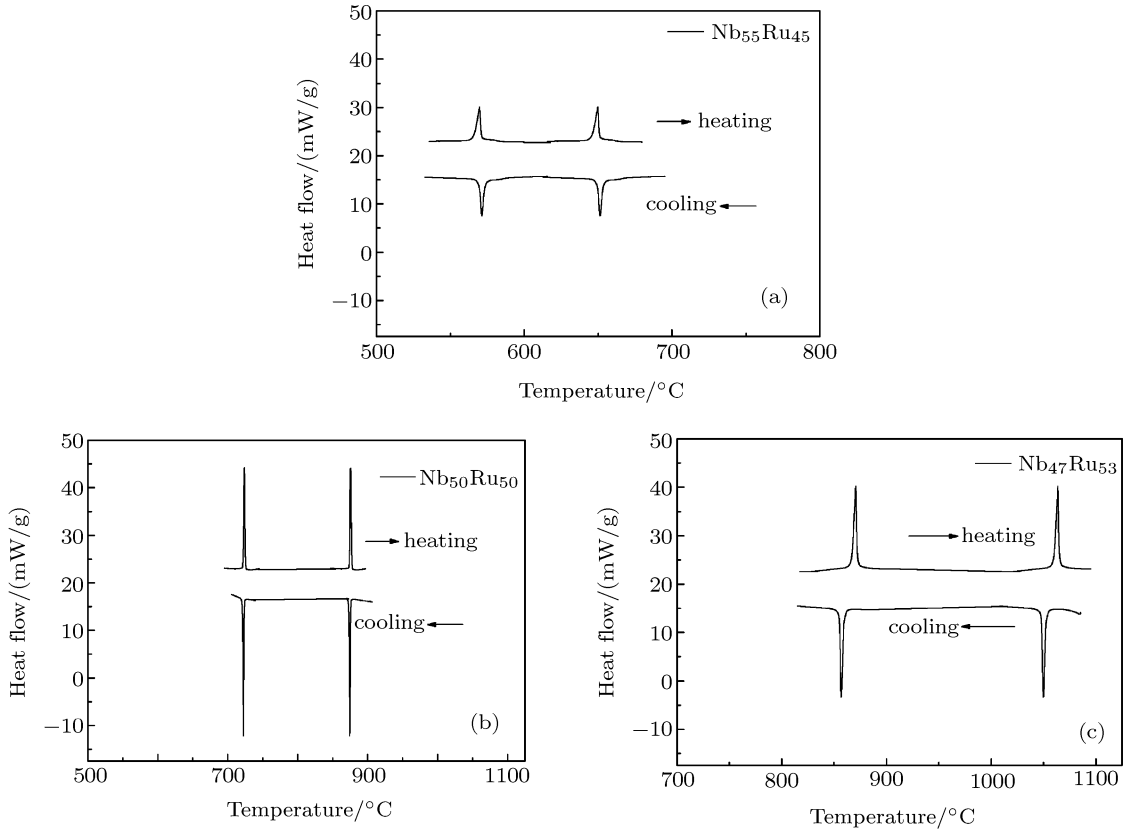


Fig. 1. DSC curves of $Nb_{50+x}Ru_{50-x}$ ($x = -3$, 0, 5) alloys: (a) $Nb_{55}Ru_{45}$, (b) $Nb_{50}Ru_{50}$, (c) $Nb_{47}Ru_{53}$.

Table 1. Characteristic temperatures of the martensitic transformation of $Nb_{50+x}Ru_{50-x}$ ($x = -3$, 0, 5) alloys.

	M_{s1}/°C	M_{f1}/°C	A_{s1}/°C	A_{f1}/°C	M_{s2}/°C	M_{f2}/°C	A_{s2}/°C	A_{f2}/°C
$Nb_{47}Ru_{53}$	1054	1037	1062	1077	863	845	870	883
$Nb_{50}Ru_{50}$	887	875	890	901	741	722	725	746
$Nb_{55}Ru_{45}$	648	629	643	668	562	544	548	563

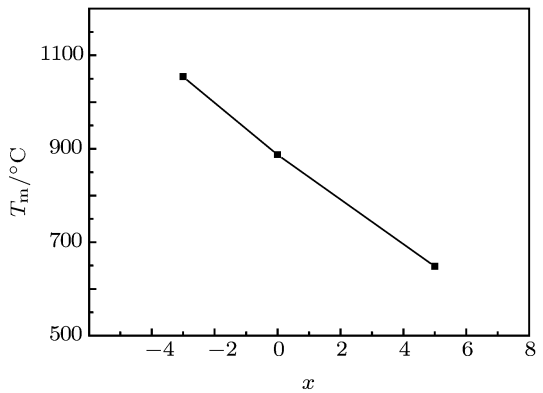


Fig. 2. Effect of Nb content on T_m of $Nb_{50+x}Ru_{50-x}$ ($x = -3$, 0, 5) alloys.

The effects of Nb content on the crystal structure and the lattice parameters of NbRu alloys at room temperature are studied by the x-ray diffraction measurement. Our results show that the space group of $Nb_{50+x}Ru_{50-x}$ β'' martensite is *Cmmm*. The monoclinic crystal remains unchanged with the content of Nb. The lattice parameters of $Nb_{50+x}Ru_{50-x}$($x = -3$, 0, 5) alloys as a function of Nb content are calculated with the help of high angle reflections of x-ray diffraction spectra as shown in Fig. 3. It is noted that the lattice parameters a, b, c and β increase slightly with increasing Nb content. This trend is attributed to the fact that the atomic radius of Nb is larger than that of Ru.

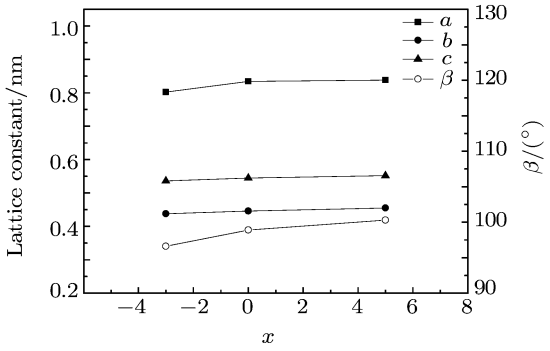


Fig. 3. Lattice parameters of $Nb_{50+x}Ru_{50-x}$ ($x = -3$, 0, 5) β'' martensite as a function of Nb content.

In order to further investigate the effects of Nb content on phase stability and martensitic transformation, the lattice contants and heats of formation for β phases of $Nb_{50+x}Ru_{50-x}$($x = -6.25$, 0, 6.25) alloys are calculated. Figure 4 shows the lattice constants as a function of Nb content for $Nb_{50+x}Ru_{50-x}$ β phases. It can be seen that the lattice constants decrease with increasing Nb content. However, the atomic size of Nb is larger than that of Ru. This abnormal decrease of lattice constants is related to the change of phase stability of $Nb_{50+x}Ru_{50-x}$ β phases. In addition, we find that the error in the calculated lattice constant compared with the experimental data for the $Nb_{50}Ru_{50}$ β phase is less than 1%,[24] demonstrating that the pseudopotentials used here and the geometry are reliable.

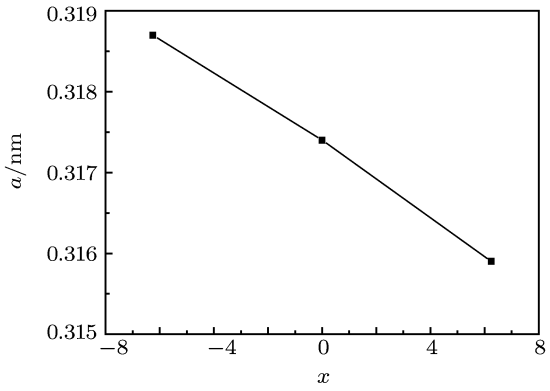


Fig. 4. Lattice parameters of $Nb_{50+x}Ru_{50-x}$($x = -6.25$, 0, 6.25) β phases as a function of Nb content.

Figure 5 clearly shows that the heat of formation of the $Nb_{50+x}Ru_{50-x}$ β phase decreases with increasing Nb content. The reduction of heats of formation for $Nb_{50+x}Ru_{50-x}$ alloys suggests that the stability of the β phase increases with increasing Nb content. For NbRu alloys, greater stability of the β phase would imply a lower β-to-β' martensitic transformation temperature. For Ni–Mn–Ga shape memory alloys, this is indeed found to be so.[25] Therefore, our results indicate that the increase of Nb content gives rise to the decrease of T_m, which is in accordance with our experimental data.

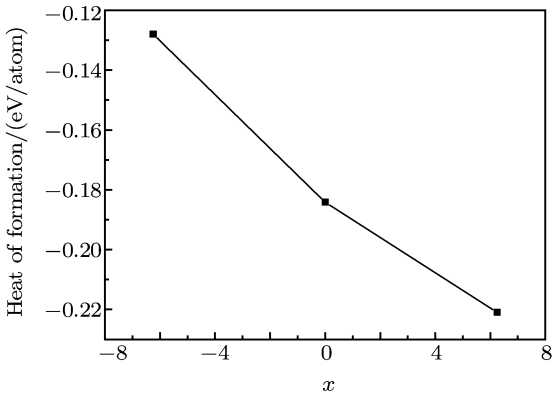


Fig. 5. Heats of formation of $Nb_{50+x}Ru_{50-x}$($x = -6.25$, 0, 6.25) β phases.

The mechanism of the effect of Nb content on phase stability can be deeply understood on the basis of density of states (DOS). Figures 6(a) and 6(b) show the total and the d partial DOSs of $Nb_{50+x}Ru_{50-x}$($x = -6.25$, 0, 6.25) β phases, respectively. For the β phase of NbRu, the total DOS resembles that of a bcc metal in that it consists of two sets of peaks separated by a dip about 1.8 eV wide. It is found that the total DOS is mainly due to d states. There are negligible contributions from the p states and the s states. The Fermi level lies in a rising part of the DOS below the higher energy peaks which are mostly unoccupied. In the case of the $Nb_{50+x}Ru_{50-x}$ β phase, the general shape of the total DOS is similar to that of NbRu. This is understandable because the shape of the DOS is mainly determined by the crystal structure. In particular, it can be seen that the dip of the total DOS for $Nb_{50+x}Ru_{50-x}$ decreases with increasing Nb content. This suggests that the β phase becomes more stable with the increase of Nb content, which is in accordance with the results of heats of formation. By comparing the d partial DOS with the atoms, it can be found that the difference is mainly due to Nb and Ru substitution. We use Nb 1 and Ru 1 to indicate the Nb and Ru atoms at the normal sites, respectively. Nb 2 and Ru 2 denote the substitution of a Nb atom for a Ru atom and the substitution of a Ru atom for a Nb atom, respectively. For $Nb_{43.75}Ru_{56.25}$, the d partial DOS for Ru 2 exhibits a clear peak near the Fermi level, significantly increasing the dip of the total DOS. In the case of $Nb_{56.25}Ru_{43.75}$, the dip of d partial DOS for Nb 2 locates at the same position as the dip of the total DOS. This contributes to the decrease of the dip of the total DOS.

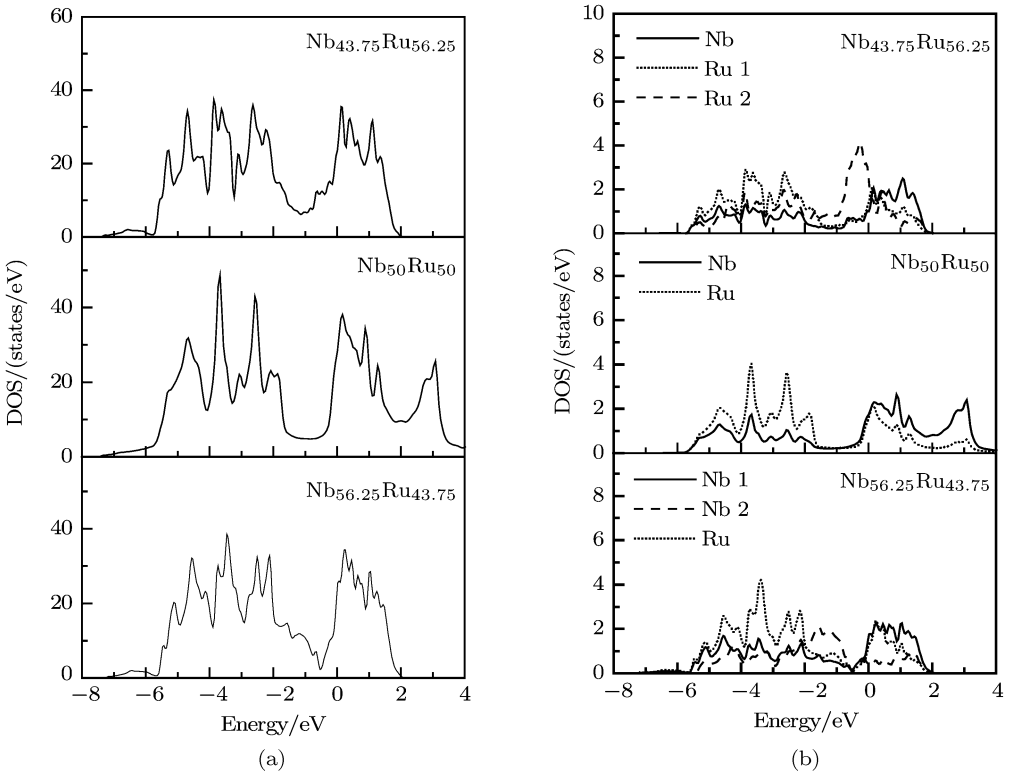


Fig. 6. DOS of $Nb_{50+x}Ru_{50-x}$ ($x = -6.25$, 0, 6.25) β phases: (a) total DOS, (b) d partial DOS of Nb and Ru.

To further study the mechanism of phase stability, the charge densities in the (110) plane of $Nb_{50+x}Ru_{50-x}$ ($x = -6.25$, 0, 6.25) β phases are calculated and shown in Fig. 7. In general, high charge accumulation between neighbouring atoms indicates a strong hybridization between the orbitals of the atoms and thus a strong bonding interaction. From Fig. 7, it can be seen that when Nb occupies the Ru sites in $Nb_{56.25}Ru_{43.75}$, there is a high charge accumulation in the interatomic areas, indicating a strong bonding interaction. In contrast, the charge accumulation between atoms is much less when Ru occupies the Nb sites in $Nb_{43.75}Ru_{56.25}$, suggesting a weaker bonding interaction, which explains why the increase of Nb content has a tendency to increase the phase stability of the β phase.

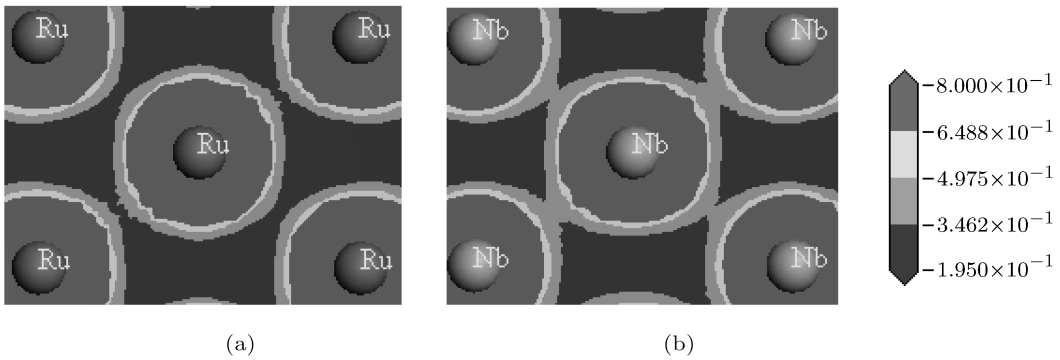


Fig. 7. Charge density of the β phase in the (110) plane: (a) $Nb_{43.75}Ru_{56.25}$, (b) $Nb_{56.25}Ru_{43.75}$.

Summarized in Table 2 are the shape memory behaviours of $Nb_{50+x}Ru_{50-x}$ ($x = -3$, 0, 5) alloys at different pre-strains. It can be seen that the recovery ratio decreases with increasing pre-strain. For the studied alloys, the maximum SME strain is 1.8%. The previous results showed that varying the Nb content could change the phase transformation type from $\beta \to \beta' \to \beta''$ to $\beta \to \beta'$. However, from Table 1, it is found that Nb content has a slight effect on the SME strain. Therefore, it can be demonstrated that the β-to-β' phase transformation is responsible for the shape memory effect in NbRu alloys.

Table 2. Shape memory behaviours of $Nb_{50+x}Ru_{50-x}$ ($x = -3$, 0, 5) alloys at different pre-strains.

	pre-strain $\varepsilon_{pre}/\%$	strain after unloading $\varepsilon_r/\%$	strain after heating $\varepsilon_p/\%$	SME strain $\varepsilon_{SME}/\%$	recovery ratio $R/\%$
$Nb_{50}Ru_{50}$	2.5	0.9	0.2	0.7	77.8
	5	3.2	1.4	1.8	43.8
	10	8.1	6.3	1.8	22.2
$Nb_{55}Ru_{45}$	2.5	0.8	0.1	0.7	87.5
	5	3.1	1.5	1.6	51.6
	10	8.0	6.2	1.8	22.5
$Nb_{47}Ru_{53}$	2.5	0.9	0.1	0.8	88.9
	5	3.3	1.6	1.7	51.5
	10	8.3	6.5	1.8	21.7

4. Conclusions

The effect of Nb content on the martenstic transformation of NbRu high-temperature shape memory alloys is studied by experimental and first-principles methods. The results show that the increase of Nb content increases the stability of $Nb_{50+x}Ru_{50-x}$ β phases, leading to the decrease of the β-to-β' martensitic transformation temperature. This provides an effective way to adjust the martensitic transformation temperature for high temperature application by varing the Nb content. The mechanism of the β phase-stabilizing effect of Nb is attributed to its dip of d partial DOS near the Fermi level, which is consistent with the analysis of heats of formation. In addition, the calculated charge densites show that Nb content plays an important role in the bonding interaction in $Nb_{50+x}Ru_{50-x}$ β phases.

References

[1] Otsuka K and Ren X 2005 *Prog. Mater. Sci* **50** 511
[2] Wayman C M 1992 *Prog. Mater. Sci.* **36** 203
[3] Xu G L, Chen J D, Chen D, Ma J Z, Yu B H and Shi D H 2009 *Chin. Phys.* B **18** 744
[4] Tan C L, Cai W and Tian X H 2006 *Chin. Phys.* **15** 2718
[5] Otsuka K and Ren X 1999 *Intermetallics* **7** 511
[6] Beyer J and Mulder J H 1995 *Mater. Res. Soc. Symp. Proc.* **360** 443
[7] Otsuka K and Wayman C M 1998 *Shape Memory Materials* (Cambridge: Cambridge University Press)
[8] Firstov G S, Humbeeck J V and Koval Y N 2004 *Mater. Sci. Eng.* A **378** 2
[9] Chastaing K, Denquin A, Portier R and Vermaut P 2008 *Mater. Sci. Eng.* A **481–452** 702
[10] He Z R, Zhou J E and Furuya Y 2003 *Mater. Sci. Eng.* A **348** 36
[11] Donkersloot H C and van Vucht J H N 1970 *J. Less-Common Met.* **20** 83
[12] Das B K, Schmerling M A and Lieberman D S 1970 *Mater. Sci. Eng.* **6** 248
[13] Scherling M A, Das B K and Lieberman D S 1970 *Metall. Trans.* **1** 3273
[14] Das B and Lieberman D S 1975 *Acta Metall.* **23** 579
[15] Das B, Stern E A and Lieberman D S 1976 *Acta Metall.* **24** 37
[16] Fonda R W, Jones H N and Vandermeer R A 1998 *Scripta Mater.* **39** 1031
[17] Fonda R W and Vandermeer R A 1997 *Philos. Mag.* A **76** 119
[18] Fonda R W and Jones H N 1999 *Mater. Sci. Eng.* A **273–275** 275
[19] Tan C L, Cai W and Tian X H 2007 *Scripta Mater.* **56** 625
[20] Tan C L, Tian X H and Cai W 2008 *Chin. Phys. Lett.* **25** 3372
[21] Gao X, Zheng Y F, Cai W, Zhang S and Zhao L C 2004 *J. Mater. Sci. Technol.* **20** 97
[22] Segall M, Lindan P, Probet M, Pickard C, Hasnip P, Clark S and Payne M 2002 *J. Phys. Condens. Matter* **14** 2717
[23] Vanderbilt D 1990 *Phys. Rev.* B **41** 7892
[24] Shapiro S M, Xu G, Gu G, Gardner J and Fonda R W 2006 *Phys. Rev.* B **73** 214114
[25] Chen J, Li Y, Shang J X and Xu H B 2006 *Appl. Phys. Lett.* **89** 231921